Oscillons, spiral waves, and stripes in a model of vibrated sand

Daniel H. Rothman

Department of Earth, Atmospheric, and Planetary Sciences, Massachusetts Institute of Technology, Cambridge, Massachusetts 02139

(Received 20 May 1997; revised manuscript received 14 October 1997)

A semicontinuum model of a thin layer of vibrated sand is proposed that qualitatively reproduces experimental observations of localized subharmonic excitations (''oscillons'') in addition to globally striped patterns. Numerical simulations recover a phase diagram similar to experimental observations and physical mechanisms for the transitions across phase boundaries are proposed. A scaling law is given for the size of the stripes and oscillons. Simulations in a different region of phase space reveal spiral waves. [S1063-651X(98)50802-1]

PACS number(s): 83.10.Pp, 83.70.Fn, 47.54.+r, 46.10.+z

This paper addresses the recent discovery by Umbanhowar, Melo, and Swinney (UMS) of novel localized subharmonic excitations in vibrated sand [1]. These excitations—dubbed ''oscillons''—are considerably different than the usual global patterns associated with nonequilibrium pattern formation [2], not only because they are local, but also because they interact. Thus, one would like to know both why they exist and whether any of the peculiarities of granular media [3] are necessary for their formation. To address these questions, this paper proposes a model, which is based partly on continuum mechanics [4] and studied by numerical simulation. In addition to recovering much of the phenomenology of the UMS experiments, the model serves to indicate a physical mechanism for the appearance of the localized excitations and their interactions. In particular, both local and global structures are seen to result from density fluctuations, which, due to the inelasticity of intergranular collisions, can create bistable states. The model also exhibits spiral waves of the type usually associated with reaction-diffusion systems [5].

The relevant experimental setting is as follows [1,6–9]. A layer of granular material (''sand''), about 15 particles deep and with two-dimensional horizontal extent far greater than its depth, is subjected to vibrations by an underlying massive plate. The vertical displacement s of the plate is sinusoidal with frequency f and amplitude A: $s(t)=A\sin 2\pi ft$. The control parameters of the experiment are f and the dimensionless acceleration $\Gamma=A(2\pi f)^2/g$, where g is the acceleration of gravity. In the oscillatory motion that results for $\Gamma>1$, subharmonic striped patterns in addition to patterns with square and hexagonal symmetry have been observed [6–9]. Oscillons appear within the same experiment [1,8]. They are confined circular regions of subharmonic oscillations of frequency $f/2$ surrounded by regions oscillating with the excitation frequency f. They occur in a small region of the Γ,f phase plane, in the transition region between patterned and flat states.

Whereas other models of vibrated sand usually consist of either microscopic molecular dynamics (e.g., [10,11]) or fully continuous amplitude equations [12], the model introduced in this paper is in a sense a combination of the physical realism of microscopic models with the convenience of continuum-mechanical approximations. In particular, the present model derives in part from the observation [7] that aspects of the transitions from one global pattern to another are contained in the dynamics of a single inelastic bouncing ball. Here this idea is generalized so that the bouncing balls are viscously coupled, weakly elastic, and capable of horizontal mass transfer. Specifically, assume that space is continuous and that the vertical extent of the sand layer may be contracted to a two-dimensional sheet with height $h(x,y,t)\geqslant s(t)$ moving in the vertical direction with velocity $u(x,y,t)$, where t is time and x and y are orthogonal coordinates in a plane parallel to the vibrating plate. The equation of motion of the sheet is

$$\partial_t u=\nu\nabla^2 u-g+B(h,u,s,\dot{s},\alpha), \tag{1}$$

where $\nabla^2=\partial_x^2+\partial_y^2$, ν is the viscosity coefficient, and the function B specifies how the sheet bounces when it hits the plate. B is implicitly defined by [13]

$$u\rightarrow\dot{s}+\alpha(\dot{s}-u)$$

when

$$h=s, \tag{2}$$

where $0<\alpha<1$ is the effective coefficient of restitution of the granular aggregate and the height h is given by $\partial_t h=u$.

The coefficient α plays a major role in the model. Although it is often assumed that grain-grain collisions cause a pile of vibrated sand to act as if the effective value of α were zero [6,7,14], *thin* layers of sand may be expected to have significant fluctuations in density that result in α varying in both space and time. Specifically, define the area density $\rho(x,y,t)$ to be the number of particles above a unit area of the vibrating plate. Density fluctuations then enter the dynamics via an ''equation of state'' $\alpha(\rho)$ that is inserted into Eqs. (1) and (2). The precise form of $\alpha(\rho)$ should be unimportant, but, following common observation [3], it should be a monotonically decreasing function of ρ.

It remains to specify how ρ evolves. First, one expects density gradients to smooth out due to self-diffusion. Second, since the sand layer is thin, h may be considered to be approximately equal to the height of the top of the layer, with $h-s$ the layer's thickness. Then when a part of the sheet $h(x,y,t)$ impacts the plate ($h=s$), sand splashes towards regions where $h>s$, that is, it moves in the direction of increasing h. Whereas the sheet—a mathematical

 © 1998 The American Physical Society

artifice—may reside on the plate for only an instant of time, real layers of finite thickness should undergo this rearrangement of mass during a significant fraction of the vibration cycle. Assuming that the gradients of both h and ρ are small, and that horizontal motion can occur at all times, a linear response gives the mass flux $\mathbf{J}=-D(\nabla\rho-\rho\nabla h/h_0)$, where D is a diffusion coefficient, h_0 is a characteristic height, and ∇ is the horizontal gradient. Conservation of mass then gives $\partial_t\rho=-\nabla\cdot\mathbf{J}$ or

$$\partial_t\rho=D[\nabla^2\rho-\nabla\cdot(\rho\nabla h/h_0)]. \tag{3}$$

Equations (1)–(3) are solved by an explicit finite difference scheme on a square lattice with periodic boundary conditions and a discrete time step equal to $10^{-2}/f$. Additionally, Newton's method is used to determine the precise time at which the bounce condition $h=s$ is met. The effective coefficient of restitution is given by

$$\alpha(\rho)=\begin{cases}\alpha_2, & \rho<\rho_1\\ \alpha_1+\dfrac{1}{2}(\alpha_2-\alpha_1)\left[1+\cos\left(\pi\dfrac{\rho-\rho_1}{\rho_2-\rho_1}\right)\right], & \rho_1<\rho<\rho_2\\ \alpha_1, & \rho>\rho_2.\end{cases}$$

In the simulations described below [except Fig. 1(d)], $\alpha_1=0.20$, $\alpha_2=0.25$, $\rho_1=0.94\rho_{\mathrm{av}}$, and $\rho_2=0.99\rho_{\mathrm{av}}$, where ρ_{av} is the average density. To aid comparison to experiments, a characteristic frequency f_0 is implicitly defined in terms of ν, D, and a characteristic grain size a by choosing $\nu/(2\pi f_0a^2)=0.03$ and $D/(2\pi f_0a^2)=0.9$, and the characteristic height h_0 is set to $16g/(2\pi f_0)^2$. Since sharp fronts are expected as a result of the impulsive forcing (2), the lattice spacing Δ is chosen to be of the order of the mean-free-path ℓ. For frequencies near f_0, one has $\ell\sim\sqrt{\nu/f_0}\simeq0.4a$; thus, Δ is set equal to a. In the UMS experiments, $a\simeq0.017$ cm and $f_0\simeq25$ Hz. Using these quantities, one finds that the simulation parameters correspond to $\nu\simeq1.4\times10^{-3}$ cm^2/s, $D\simeq4.1\times10^{-2}$ cm^2/s, and $h_0\simeq0.64$ cm$\simeq2.2na$, where $n=17$ is a typical number of particles in a layer.

Figure 1 depicts steady patterns of the field $h(x,y)$ obtained from simulations performed with different control parameters. Since a flat interface is linearly stable, simulations are initialized far from the flat state, with randomly distributed h and u and uniform ρ. The transient evolution of the system (not shown) is such that fluctuations in h lead to fluctuations in ρ, allowing small areas of low density, and thus large α, to form. One example of the eventual steady solution, for $\Gamma=2.42$ and $f/f_0=1.06$, is depicted in Fig. 1(a). The small circular regions of black or white are ''oscillons'' oscillating subharmonically with frequency $f/2$, while the gray area is oscillating with the excitation frequency f. Note that two oscillons of opposite polarity occur as a bound pair, similar to the interactions found in the UMS experiments [1,8].

Figure 2 shows a three-dimensional perspective of one isolated oscillon and the bound pair in Fig. 1(a) at an integer value of $\tau=ft$. The time variation of h and ρ inside and outside the isolated oscillon is also shown. One sees clearly that the oscillon is subharmonic, with craters changing to peaks, or peaks changing to craters, once per vibration cycle upon impact with the plate. Moreover, the mechanism for the oscillon's excitation is clear: when the crater phase impacts the plate (e.g., at $\tau\simeq1$), the density is low, and the bounce is correspondingly high. When the peak hits the plate, however, the density is high and the bounce low. The time-averaged density within the oscillon is ρ_{av}, the same density as its environment. This behavior is qualitatively different than that found in the model of Ref. [12], which predicts that the time-averaged density within oscillons is significantly decreased.

Figure 1(b) depicts another stationary state of the model, a stable pattern of randomly oriented stripes oscillating subharmonically with frequency $f/2$. The parameters of this simulation are the same as for Fig. 1(a), except that now $f/f_0=0.96$. The transient evolution to this pattern is similar to

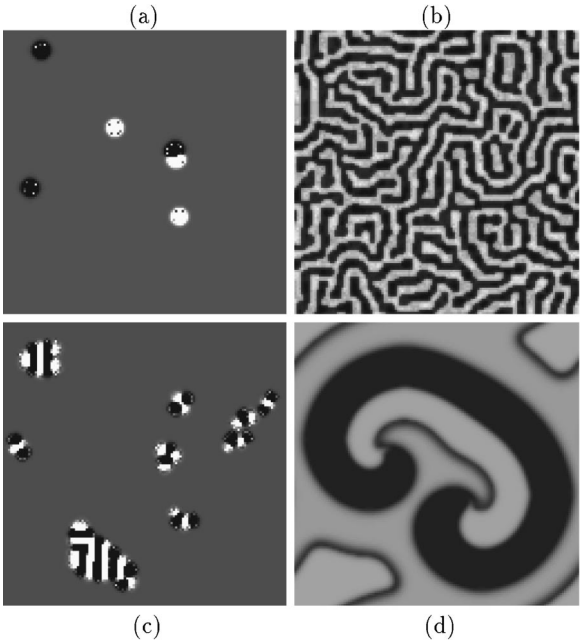

FIG. 1. Steady patterns of the height field $h(x,y)$; the grey scale indicates relative height (white is high) and the lattice size is 128^2 in all cases. Contrast is exaggerated for clarity. (a): Oscillons ($\Gamma=2.42$, $f/f_0=1.06$). (b): Stripes ($\Gamma=2.42$, $f/f_0=0.96$). (c): Tangled oscillons ($\Gamma=2.34$, $f/f_0=0.96$). (d): Spiral wave oscillating with frequency $f/3$ ($\Gamma=9.0$, $f/f_0=1.0$; see text for other parameters).

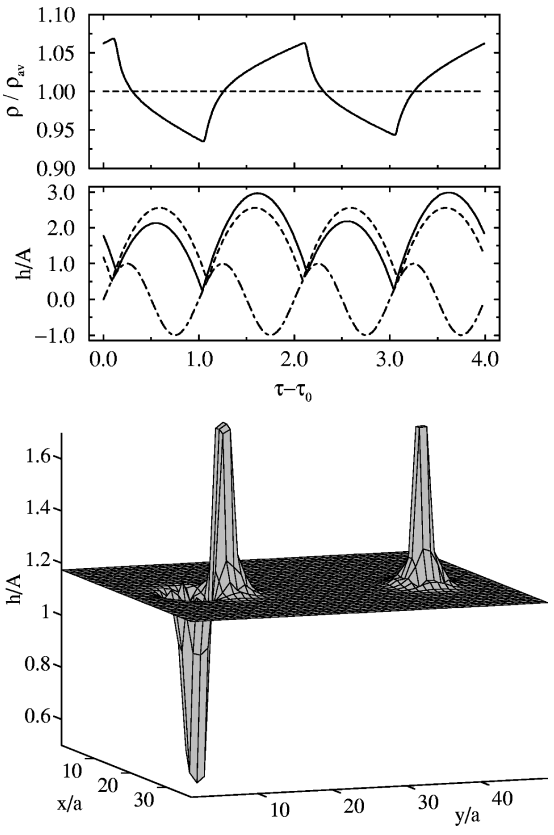

FIG. 2. Bottom: Three-dimensional perspective of the two bound oscillons and one of the isolated oscillons of Fig. 1, at time $\tau=\tau_0$, an integer. Top: Evolution of $h(t)$ and $\rho(t)$ inside (solid line) and outside (dashed line) the isolated oscillon in addition to the plate motion $s(t)$ (dotted-dashed line).

the sequence described for Figs. 1(a) and 1(b), except that the oscillons that are formed, particularly those which are paired, are unstable. Patches of striped regions then grow, eventually filling the entire space. Figure 1(c), on the other hand, shows that for the same frequency but with $\Gamma=2.34$, this growth terminates in the form of localized stable subharmonic *tangled oscillons* with frequency $f/2$. The tangled oscillons occur as either stable chains of oscillons or as localized stripes. Both cases have been observed in experiments [1,8].

These simulations and others are summarized in the phase diagram of Fig. 3. One sees that the oscillon phase is sandwiched between the striped and flat phases in the plane of the control parameters Γ and f. A comparison with the phase diagram of the UMS experiments [1] reveals two important similarities. First, the values of Γ over which the oscillons are observed is roughly the same. Second, in both cases the transition from a globally patterned state—here, stripes, while in the UMS experiments, standing waves with square symmetry— to oscillons to the flat state occurs generally as Γ decreases or f increases. That the dependence on Γ so closely matches experiments is partly the result of the choice of α_1 and α_2. The values chosen here span a bifurcation from period-1 to period-2 oscillations of a single bouncing ball. Decreasing α_1 and α_2 would increase the values of Γ over which oscillons are observed. Thus the match in Γ suggests that the UMS sand layer has an *effective* coefficient of restitution of $\alpha\simeq 0.2$.

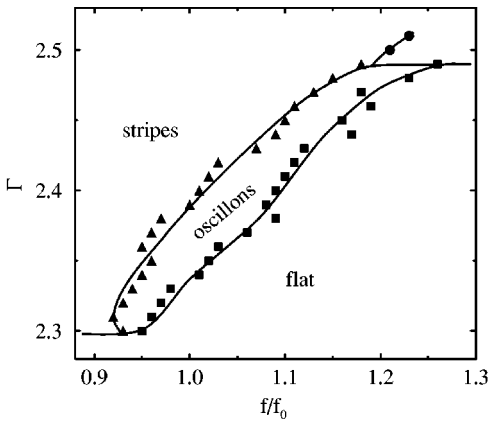

FIG. 3. Phase diagram detailing the appearance of stable stripes, oscillons, and flat states. The tangled oscillon phase (not labeled) occurs in the part of the oscillon region where $\Gamma<2.37$. Squares: Transitions between oscillons and flat state. Triangles: Transitions between stripes and oscillons. The circles separate stripes from complex period-2 structures.

The radius of the oscillons and width of the stripes is chosen by the diffusivity D: increasing D while holding f constant increases the length over which material can move horizontally, for example, into and out of an oscillon. This length, which should scale like $(D/f)^{1/2}$, determines the size of the area over which ρ (and thus α) may fluctuate. Figure 4 confirms this argument. The length scale Λ is computed from the peak of the circularly averaged two-dimensional power spectrum of $h(x,y)$, in the same manner as is commonly employed in studies of domain growth [15].

The transitions in Fig. 3 may now be explained. From Eq. (3), one sees that the amplitude $\Delta\rho_{\rm in}$ of the density fluctuations inside an oscillon should scale such that

$$\Delta\rho_{\rm in}/\rho_{\rm av}\sim D/(a^2 f)\sim(f_0/f). \tag{4}$$

Thus, for constant Γ there is a critical frequency f_c above which $\Delta\rho_{\rm in}$ becomes too small to excite subharmonic oscillations, or, in other words, the oscillons decay into the flat

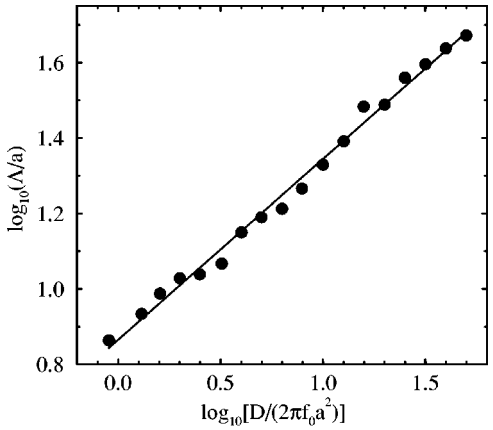

FIG. 4. Characteristic length scale Λ, proportional to the stripe width, for varying values of the diffusivity D, computed with $\Gamma=2.42$ and $f/f_0=1.0$. The straight line, obtained from linear regression, has slope 0.48 ± 0.01, which compares well to the predicted value of 1/2.

phase. To understand the transition from oscillons to stripes, note that the difference between the amplitude of the density fluctuations a small distance $\ell \sim a$ inside and outside an oscillon of radius R should scale like ℓ/R due to the conservation of mass. In symbols,

$$(\Delta\rho_{\rm in}-\Delta\rho_{\rm out})/\rho_{\rm av}\sim \ell/R\sim (a^2 f/D)^{1/2}\sim (f/f_0)^{1/2}.$$

Thus as f decreases $\Delta\rho_{\rm in}$ and $\Delta\rho_{\rm out}$ approach one another. There is then a critical frequency $f_c'<f_c$ below which the density fluctuations are sufficient to excite subharmonic oscillations both inside *and* outside an oscillon—that is, form stripes—but above which an isolated oscillon may be stable. Note that this argument also explains why oscillons often occur in out-of-phase pairs or chains, since these structures are essentially nascent stripes whose further growth is frustrated due to large f. The argument also makes clear why the transition from oscillons to stripes is one in which a global pattern is formed not by the instability of a particular mode, but rather by the filling of space by a particular localized pattern [16].

The pattern of Fig. 1(d), a snapshot of an expanding spiral wave [5] in which each band of constant height is oscillating with frequency $f/3$, is qualitatively different from the others. Compared to the patterns discussed above, here the excitation is much greater ($\Gamma=9.0$) as is the viscosity [$\nu/(2\pi f a^2)=0.4$], and the sheet is more inelastic ($\alpha_1=0.0$ and $\alpha_2=0.05$). The other parameters are unchanged. Much the same behavior is also obtained by setting $D=0$, in which case stable spiral waves of period 3 are found for $9.0<\Gamma<10.0$. Such spiral waves are well known solutions [5] of coupled nonlinear oscillators such as those represented by Eq. (1). Spiral patterns that are probably of a different nature have recently been observed in experiments [8].

In concluding, it is useful to emphasize that the model of this paper is based explicitly on the inelasticity of intergranular collisions. Thus, although broadly similar structures have been found in vibrated liquids [17], the mechanisms detailed here do not appear to have a direct physical analog in incompressible fluids. On the other hand, several Ginzburg-Landau or amplitude-equation models have been proposed as universal models of localized excitations [12,18–20]. Although these models are less mechanistic than the one here, they are simpler, in part because they represent an averaging over both time and space, whereas the model of this paper is essentially microscopic in time. It is likely that a full continuum-mechanical approximation of Eqs. (1)–(3) exists. Its specification is an important open question because it will not only aid comparison with Refs. [12,18–20] but will also help identify other systems in which localized excitations are possible.

It is a pleasure to thank Michael Brenner for helpful discussions. I would also like to thank P. Dodds, J. Feder, O. van Genabeek, S. Nagel, P. Umbanhowar, and T. Witelski for their remarks. This work was supported in part by NSF Grant No. EAR-9706220.

[1] P. B. Umbanhowar, F. Melo, and H. L. Swinney, Nature (London) **382**, 793 (1996).
[2] M. C. Cross and P. C. Hohenberg, Rev. Mod. Phys. **65**, 851 (1993).
[3] H. M. Jaeger, S. R. Nagel, and R. P. Behringer, Rev. Mod. Phys. **68**, 1259 (1996).
[4] P. K. Haff, J. Fluid Mech. **134**, 401 (1983).
[5] J. D. Murray, *Mathematical Biology*, 2nd ed. (Springer-Verlag, New York, 1993).
[6] F. Melo, P. B. Umbanhowar, and H. L. Swinney, Phys. Rev. Lett. **72**, 172 (1994).
[7] F. Melo, P. B. Umbanhowar, and H. L. Swinney, Phys. Rev. Lett. **75**, 3838 (1995).
[8] P. B. Umbanhowar, F. Melo, and H. L. Swinney, Physica A (to be published).
[9] T. H. Metcalf, J. B. Knight, and H. M. Jaeger, Physica A **236**, 202 (1997).
[10] K. M. Aoki and T. Akiyama, Phys. Rev. Lett. **77**, 4166 (1996).
[11] C. Bizon *et al.*, Phys. Rev. Lett. (to be published).
[12] L. Tsimring and I. Aranson, Phys. Rev. Lett. **79**, 213 (1997).
[13] J. Guckenheimer and P. Holmes, *Nonlinear Oscillations, Dynamical Systems, and Bifurcations of Vector Fields* (Springer-Verlag, New York, 1983).
[14] S. Douady, S. Fauve, and C. Laroche, Europhys. Lett. **8**, 621 (1989).
[15] J. Gunton, M. S. Miguel, and P. Sahni, in *Phase Transitions and Critical Phenomena*, edited by C. Domb and J. L. Lebowitz (Academic Press, New York, 1983), Vol. 8, pp. 269–482.
[16] F. Melo and S. Douady, Phys. Rev. Lett. **71**, 3283 (1993).
[17] O. Lioubashevski, H. Arbell, and J. Fineberg, Phys. Rev. Lett. **76**, 3959 (1996).
[18] O. Thual and S. Fauve, J. Phys. (France) (France) **49**, 119 (1988).
[19] I. S. Aranson, K. A. Gorshkov, A. S. Lomov, and M. I. Rabinovich, Physica D **43**, 435 (1990).
[20] R. J. Deissler and H. R. Brand, Phys. Rev. A **44**, R3411 (1991).